



**Universiteit
Leiden**
The Netherlands

Imaging of coronary atherosclerosis and vulnerable plaque

Velzen, J.E. van

Citation

Velzen, J. E. van. (2012, February 16). *Imaging of coronary atherosclerosis and vulnerable plaque*. Retrieved from <https://hdl.handle.net/1887/18495>

Version: Corrected Publisher's Version

License: [Licence agreement concerning inclusion of doctoral thesis in the Institutional Repository of the University of Leiden](#)

Downloaded from: <https://hdl.handle.net/1887/18495>

Note: To cite this publication please use the final published version (if applicable).



CHAPTER 2

Evaluation of Coronary Plaque
Type and Composition with 320-
Row Multidetector Computed
Tomography: Comparison to Virtual
Histology Intravascular Ultrasound

Joëlla E. van Velzen, Joanne D. Schuijf, Fleur R. de Graaf, Mark J. Boogers,
Cornelis J. Roos, Martin J. Schalij, Lucia J. Kroft, Albert de Roos, Johan H.C.
Reiber, Ernst E. van der Wall, J. Wouter Jukema, Jeroen J. Bax

Education in Heart, in press

ABSTRACT

Background: Recently, 320-row multidetector computed tomography angiography (CTA) has been introduced. However, the relation between plaque observations on 320-row CTA versus virtual histology intravascular ultrasound (VH IVUS) remains relatively unknown. Therefore, the objective of this study was to compare plaque observations on 320-row CTA to VH IVUS.

Methods: In total, 65 patients underwent 320-row CTA followed by VH IVUS. On CTA, three plaque types were identified: non-calcified, mixed and calcified. Attenuation values (Hounsfield Units (HU)) were measured in 3 regions of interest. On VH IVUS, plaque composition (% fibrotic, fibro-fatty, necrotic core, dense calcium) and presence of thin cap fibroatheroma (TCFA, more high risk) were evaluated.

Results: Overall, of the 272 plaques identified on CTA, 110 plaques (40%) were non-calcified, 142 plaques were mixed (52%) and 20 plaques (8%) were calcified. Non-calcified plaques demonstrated the lowest attenuation values (70 ± 37 HU), followed by mixed plaques (258 ± 219 HU) and calcified plaques (836 ± 226 HU). Plaque classification on CTA showed good agreement to VH IVUS. As compared with calcified plaques, non-calcified plaques contained more fibro-fatty tissue ($54 \pm 23\%$ versus $47 \pm 21\%$, $p=0.001$). Moreover, mixed and calcified plaques contained more dense calcium ($9 \pm 6\%$ and $10 \pm 7\%$, respectively) than non-calcified plaques ($6 \pm 6\%$, $p<0.001$). More necrotic core was present in mixed plaque ($16 \pm 8\%$) than in non-calcified ($12 \pm 7\%$) and calcified plaques ($14 \pm 7\%$) ($p<0.001$). Interestingly, mixed plaques most often corresponded to the presence of TCFA on VH IVUS (22%).

Conclusion: Plaque observations on 320-row CTA show good agreement to relative plaque composition on VH IVUS. Moreover, mixed plaques on 320-row CTA parallel the more high risk plaques on VH IVUS.

INTRODUCTION

Coronary multidetector computed tomography angiography (CTA) has generated great interest in recent years. The technique has been shown to have a high diagnostic performance in the non-invasive assessment of patients with known or suspected coronary artery disease (CAD).¹⁻³ An important advantage of coronary CTA is that not only luminal narrowing can be visualized but also atherosclerotic plaque composition in the arterial wall. Indeed, three different plaque types can be distinguished by CTA: non-calcified, mixed and calcified plaque. Interestingly, certain plaque characteristics on CTA have been associated with acute coronary syndromes. For instance, the presence of non-calcified and mixed coronary plaques has been related to acute coronary syndromes (ACS), whereas calcified plaques were related to stable CAD.⁴ Nonetheless, plaque characterization with CTA has been notoriously demanding, particularly with earlier generation CTA systems because of limited spatial and temporal resolution.

Recently, a novel CTA system has been introduced equipped with 320-detector rows which can provide 16-cm anatomical coverage in one gantry rotation.⁵ Accordingly, the 320-row system allows a volumetric scanning approach, covering the entire heart in a single heart beat. Additionally, volume scanning eliminates the problem of stair-step artifacts caused by inter-heartbeat variations as well as a reduction in cardiac motion artifacts often observed during step-and-shoot acquisition techniques and helical imaging. More importantly, volume scanning offers a distinct decrease in radiation dose and contrast administration in comparison with traditional helical scanning, as only one gantry rotation is needed to image the entire heart (350 ms).^{6,7} Moreover, contrast is more homogeneously distributed through the coronary arteries, thereby potentially improving the ability and reliability to characterize plaque composition.⁸ Accordingly, these developments have resulted in overall improved image quality and diagnostic accuracy for the detection of CAD.^{6,7}

However, no previous literature concerning the ability of plaque characterization in vivo with the new 320-detector row CTA technique has been published. Therefore, the aim of the present study was to evaluate the accuracy of coronary plaque characterization by the novel non-invasive 320-row CTA as compared to findings of invasive virtual histology intravascular ultrasound (VH IVUS).

METHODS

Patients and study protocol

The study group consisted of 65 symptomatic patients who presented at the outpatient clinic for the evaluation of chest pain and underwent non-invasive 320-row CTA followed by invasive coronary angiography and VH IVUS of 1 to 3 vessels. No interventions or changes in the clinical condition of the patients occurred between the examinations. Contra-indications for CTA were 1) (supra) ventricular arrhythmias, 2) renal insufficiency (glomerular filtration rate <30 ml/min), 3) known allergy to iodine contrast material, 4) severe claustrophobia, 5) pregnancy. Exclusion criteria for IVUS were severe vessel tortuosity, severe stenosis or vessel occlusion.

CTA

Data acquisition

CTA was performed using a 320-row CTA scanner (Aquilion ONE, Toshiba Medical Systems, Otawara, Japan) with 320 detector rows (each 0.50 mm wide) and a rotation time of 350 ms resulting in a spatial resolution of 0.5 mm and temporal resolution of 175 ms for half reconstruction. Beta-blocking medication (metoprolol 50 or 100 mg, single dose, 1 hour prior to CTA examination) were administered if the heart rate was ≥ 65 beats/min, unless contra-indicated. In addition, nitroglycerin (0.4 or 0.8 mg sublingual) was administered 5 minutes prior to CTA examination. For the 320-row contrast enhanced scan the entire heart was imaged in a single heartbeat, with a maximum of 16 cm cranio-caudal coverage, using prospective ECG triggering. The phase window was adjusted according to the heart rate: if the heart rate was ≥ 60 beats/min the phase window was opened at 65-85% of R-R interval, if the heart rate was stable and < 60 beats/min the phase window was opened at 70-80% of R-R interval. Tube voltage and current were adapted to body mass index (BMI) and thoracic anatomy. Tube voltage was 100 kV (BMI < 23 kg/m²), 120 kV (BMI, 23-35 kg/m²), or 135 kV (BMI > 35 kg/m²) and maximal tube current was 400-580 mA (depending on body weight and thoracic anatomy). Contrast material was administered in a triple-phase protocol: first a bolus of 60 to 80 ml, followed by 40 ml of a 50:50 mixture of contrast and saline, followed by saline flush with a flow rate of 5-6 ml/sec (Iomeron 400®, Bracco, Milan, Italy). Automatic bolus arrival detection was applied in the left ventricle with a threshold of +180 Hounsfield Units. All images were acquired during an inspiratory breath-hold of approximately 4-8 seconds. Firstly, a data set was reconstructed at 75% of R-R interval, with a slice thickness of 0.50 mm and a reconstruction interval of 0.25 mm. In case of motion artifacts, multiple phases were reconstructed to obtain maximal diagnostic image quality. Subsequently, raw data sets were transferred to a remote workstation (Vitrea FX 1.0, Vital Images, Minnetonka, MN, USA). Radiation dose was quantified with a dose-length product conversion factor of 0.014 mSv/(mGy x cm).⁹ As previously described, if scanning was performed prospectively full dose at 70-80% of R-R interval, estimated mean radiation dose was 3.9 ± 1.3 mSv (range 2.7-6.2 mSv).¹⁰ When scanning prospectively full dose at 65-85% of R-R interval, estimated mean radiation dose was 6.0 ± 3.0 mSv (range 3.1-11.8 mSv).

Coronary plaque assessment

For data evaluation, 320-row CTA angiographic examinations were evaluated by 2 experienced readers including an interventional cardiologist blinded to conventional coronary angiography and VH IVUS findings. Agreement between observers was achieved in consensus. Firstly, general information on the coronary anatomy was obtained by evaluating three-dimensional volume rendered reconstructions. Secondly, the coronary arteries were evaluated using axial images, curved multiplanar reconstructions and maximum intensity projections. Furthermore, the coronary arteries were divided into segments according to the modified American Heart Association classification.¹¹ Each segment was evaluated

for the presence of any atherosclerotic plaque (defined as structures $>1 \text{ mm}^2$ within and/or adjacent to the coronary artery lumen, which could be clearly distinguished from the vessel lumen).¹² Per segment one coronary plaque was selected at the site of the most severe luminal narrowing. Subsequently, axial slices were visually examined for the presence of significant luminal narrowing by determining the presence of $\geq 50\%$ reduction of luminal diameter. To describe plaque composition, plaques were further classified as: 1) non-calcified plaque (plaques with lower CTA attenuation values as compared to contrast-enhanced lumen without any calcification), 2) mixed plaque (non-calcified and calcified elements in single plaque) 3) calcified plaque (plaques with high CTA attenuation values as compared to contrast-enhanced lumen). Of note, very small calcifications can still be missed by CTA.¹³ As previously described, a good intra-observer agreement was observed for the classification of plaque type on CTA.^{14 15} Furthermore, within the plaque, the CTA attenuation values measurements in Hounsfield Units (HU) were made using 3 circular regions of interest (area of 1.5 mm^2) that were placed in the center of the plaque. Consequently, the mean attenuation values (HU) were determined per plaque.

VH IVUS

Image acquisition

A dedicated IVUS-console (Volcano Corporation, Rancho Cordova, CA, USA) was used for the examination. Intracoronary nitrates were administered prior to insertion of the IVUS catheter. VH IVUS was performed with a 20 MHz, 2.9 F phased-array IVUS catheter, (Eagle Eye, Volcano Corporation, Rancho Cordova, CA, USA) which was introduced distally in the coronary artery. A cine run was made before and after contrast injection to record the starting position of the IVUS catheter. Subsequently, motorized automated IVUS pullback was performed using a speed of 0.5 mm/s until the catheter reached the guiding catheter. Radiofrequency signals were collected at the R wave and images were stored on CD-ROM or DVD for off-line analysis. Of note, the typical resolution of a 20 MHz IVUS catheter is 80 microns axially and $200 \text{ to } 250 \text{ microns}$ laterally.¹⁶

Coronary plaque assessment

Offline analysis of the VH IVUS images was performed using dedicated software (pcVH 2.1 and VIAS 3.0, Volcano Corporation, Rancho Cordova, CA, USA). The lumen and the media-adventitia interface were defined by automatic contour detection and on all individual frames manual editing was performed. The four plaque components were differentiated into different color-codes (fibrotic tissue labeled in dark green, fibro-fatty in light green, necrotic core in red and dense calcium in white), as validated previously.¹⁷ For each target plaque, plaque length was measured (mm).¹⁶ Furthermore, plaques were visually qualitatively classified on 3 consecutive frames at the minimal lumen area site. Classification was obtained according to the following categorization:

- (i) Pathological intimal thickening; defined as a mixture of fibrous and fibro-fatty tissues, a plaque burden $\geq 40\%$ and $< 10\%$ necrotic core and dense calcium.
- (ii) Fibroatheroma; defined as having a plaque burden $\geq 40\%$ and a confluent necrotic core occupying 10% of the plaque area or greater in 3 successive frames with evidence of an overlying fibrous cap.
- (iii) TCFA; defined as a lesion with a plaque burden $\geq 40\%$, the presence of confluent necrotic core of $> 10\%$, and no evidence of an overlying fibrous cap in 3 successive frames.
- (iv) Fibrocalcific plaque; defined as a lesion with a plaque burden $\geq 40\%$, being mainly composed of fibrotic tissue, having dense calcium $> 10\%$ and a confluent necrotic core of $< 10\%$ (higher amount accepted if necrotic core was located exclusively behind the accumulation of calcium).^{18 19}

Statistical analysis

For each plaque type on CTA, the number and mean CTA attenuation values were assessed. On VH IVUS, relative plaque composition and plaque type was also assessed for each lesion. After initial plaque assessment, plaques on CTA were matched to plaques on VH IVUS using landmarks such as coronary ostia, side-branches and calcium deposits to allow accurate comparison between CTA and VH IVUS. Distances from the landmarks to the lesion were measured on curved multiplanar reconstructions on CTA and matched with the longitudinal images of VH IVUS. Plaque type classification on 320-row CTA was compared to both plaque composition and plaque type on VH IVUS. Finally, mean CTA attenuation values were compared between the various plaque types as assessed on VH IVUS. Continuous values were expressed as means (\pm standard deviation) and differences in plaque composition, type and Hounsfield units were assessed using a nested analysis of variance (ANOVA). Categorical values are expressed as number (percentages) and compared between groups with 2-tailed Chi-square test. A p-value of < 0.05 was considered statistically significant. Statistical analysis was performed using SPSS 16.0 software (SPSS Inc., Chicago, Illinois).

RESULTS

Patient characteristics

The CTA and VH IVUS examinations were performed without complications in 65 patients. However, 3 patients were excluded due to non-diagnostic CTA image quality as a result of motion artifacts ($n=2$) and occurrence of an ectopic heart beat ($n=1$). Baseline patient characteristics of the remaining 62 patients are presented in Table 1. Mean heart rate was 57 ± 7 beats/min. In total, 272 plaques were identified in which comparison between 320-row CTA and VH IVUS was possible. Fifty plaques (18%) corresponded to significant luminal narrowing on CTA.

Table 1. Patient characteristics of study population

	n (%)
Gender (M/F)	46 / 16
Age (years)	58 ±10
Risk factors for CAD	
Diabetes	13 (21%)
Hypertension	35 (57%)
Hypercholesterolemia	22 (36%)
Positive family history	31 (50%)
Current smoking	21 (34%)
Obese (BMI ≥30 kg/m ²)	9 (15%)
Previous CAD	
Previous myocardial infarction	15 (24%)
Previous PCI	16 (26%)
Heart rate (beats/min) during CTA	57 ±7

CAD; coronary artery disease, BMI; body mass index, PCI; percutaneous coronary intervention, CTA; multidetector computed tomography angiography.

Baseline 320-row CTA and VH IVUS results

Overall, of the 272 plaques identified on CTA, 110 plaques (40%) were non-calcified, 142 plaques were mixed (52%) and 20 plaques (8%) were calcified. Mean CTA attenuation value of the plaques was 224 ±222 HU. Non-calcified plaques demonstrated the lowest attenuation values (70 ±37 HU), followed by mixed plaques (258 ±219 HU) and calcified plaques (836 ±226 HU) (Figure 1).

VH IVUS examinations were acquired during invasive coronary angiography in 153 of the 186 available vessels (right coronary artery=51, left anterior descending coronary artery=56, left circumflex coronary artery=46). On VH IVUS, mean lesion length was 27.5 ±17.5 mm. Furthermore, the most prevalent plaque component was fibrotic tissue (52

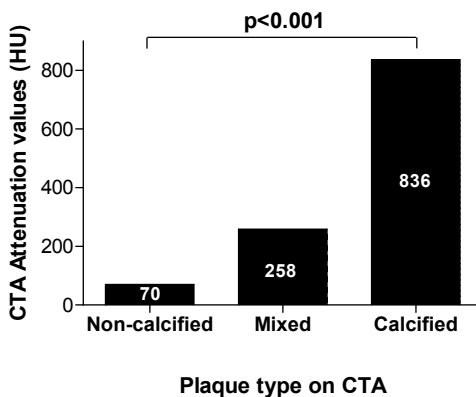


Figure 1. Comparison of attenuation values as measured in Hounsfield Units (HU) on 320-row multidetector computed tomography angiography (CTA) between the different plaque types on CTA. A significant difference in CTA attenuation values is demonstrated between non-calcified, mixed and calcified plaques on CTA ($p < 0.001$).

$\pm 18\%$), followed by fibro-fatty tissue ($28 \pm 14\%$), necrotic core ($14 \pm 8\%$) and dense calcium ($8 \pm 6\%$). The more vulnerable plaque type (TCFA) was present in 44 plaques (16%).

Comparison between 320-row CTA and VH IVUS

A good agreement was found when comparing plaque type classification on 320-row CTA to plaque composition on VH IVUS as demonstrated in Table 2. As compared with calcified plaques, non-calcified plaques contained significantly more fibro-fatty tissue on VH IVUS ($54 \pm 23\%$ versus $47 \pm 21\%$ in calcified plaques, $p=0.001$). Moreover, mixed and calcified plaques on CTA contained significantly more dense calcium ($9 \pm 6\%$ and $10 \pm 7\%$, respectively) on VH IVUS than non-calcified plaques ($6 \pm 6\%$, $p<0.001$). In addition, signifi-

Table 2. Comparison between plaque composition on virtual histology intravascular ultrasound (VH IVUS) and 320-row multidetector computed tomography angiography (CTA)

VH IVUS characteristics	Non-calcified plaques on CTA	Mixed plaques on CTA	Calcified plaques on CTA	p-value
Lesion length (mm)	29 ± 20	27 ± 16	24 ± 15	0.64
Fibrotic (%)	54 ± 23	51 ± 16	47 ± 21	0.001
Fibro-fatty (%)	18 ± 15	18 ± 13	20 ± 13	0.62
Necrotic Core (%)	12 ± 7	16 ± 8	14 ± 7	<0.001
Dense Calcium (%)	6 ± 6	9 ± 6	10 ± 7	<0.001

VH IVUS, virtual histology intravascular ultrasound; CTA, multidetector computed tomography angiography

cantly more necrotic core was present in mixed plaque ($16 \pm 8\%$) than in non-calcified ($12 \pm 7\%$) and calcified plaques ($14 \pm 7\%$) ($p<0.001$). Example of plaque evaluation on 320-row CTA as compared to VH IVUS is shown in Figure 2.

The results comparing plaque types on CTA against qualitatively assessed plaque types on VH IVUS are reported in Table 3. As expected, pathological intimal thickening on VH IVUS was most often observed in non-calcified plaques (20 (21%)) as compared to mixed plaques (14 (9%), $p=0.03$) and calcified plaques (0 (0%)) on CTA. Interestingly, the more high risk plaques on VH IVUS (TCFA) were most often observed in mixed plaques on CTA (22%, Figure 3). Moreover, fibrocalcific plaques on VH IVUS were most often observed in the calcified plaques (9 (47%) versus 5 (5%) in non-calcified, $p<0.001$) on CTA.

Furthermore, mean CTA attenuation values were compared between the different plaque types as assessed on VH IVUS (Figure 4). As shown, the more advanced plaque types on VH IVUS corresponded to higher CTA attenuation values. Pathological intimal thickening had the lowest mean attenuation value of 141 ± 124 HU, followed by the fibroatheroma (mean attenuation value of 209 ± 205 HU), TCFA (mean attenuation value of 251 ± 222) and in the fibrocalcific plaques (mean attenuation value of 387 ± 293 HU) the highest attenuation values were found. Interestingly, CTA attenuation value measure-

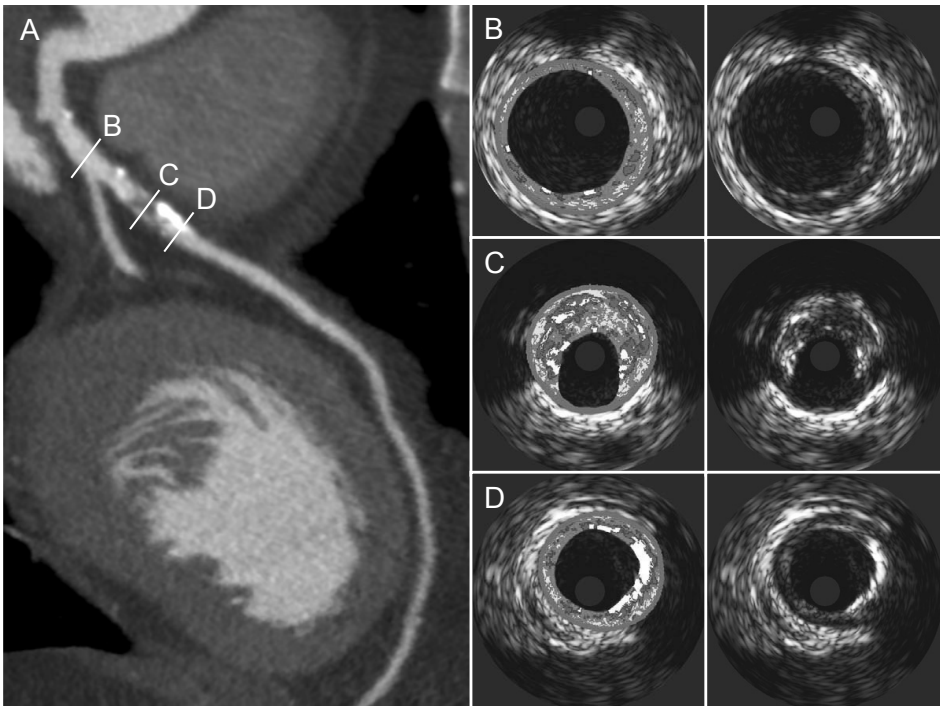


Figure 2. Example of comparison between plaque composition on 320-row multidetector computed tomography angiography (CTA) and virtual histology intravascular ultrasound (VH IVUS). In panel (A), a curved multiplanar reconstruction of the left anterior descending coronary artery is shown demonstrating no plaque at cross-section B and a mixed plaque at cross-section C and D. In panel (B, C and D) corresponding grayscale and VH IVUS images are shown. In panel (B), only minor intimal thickening is demonstrated. In panel (C), a plaque with a large plaque burden ($\geq 40\%$), large necrotic core ($\geq 10\%$) and no evidence of a fibrous cap is shown, suggesting the presence of a thin cap fibroatheroma. In panel (D) another cross-section is demonstrated showing extensive calcifications on both CTA and VH IVUS images.

Table 3. Comparison between plaque type on virtual histology intravascular ultrasound (VH IVUS) and 320-row multidetector computed tomography angiography (CTA)

VH IVUS plaque type	Non-calcified plaques on CTA	Mixed plaques on CTA	Calcified plaques on CTA	p-value
Presence PIT	20 (21%)	14 (9%)	0 (0%)	0.03
Presence FA	58 (62%)	73 (52%)	8 (42%)	0.58
Presence TCFA	11 (10%)	31 (22%)	2 (10%)	0.03
Presence FC	5 (5%)	23 (16%)	9 (47%)	<0.001

VH IVUS, virtual histology intravascular ultrasound; CTA, multidetector computed tomography; PIT, pathological intimal thickening; FA, fibroatheroma; TCFA, thin cap fibroatheroma; FC, fibrocalcific plaque

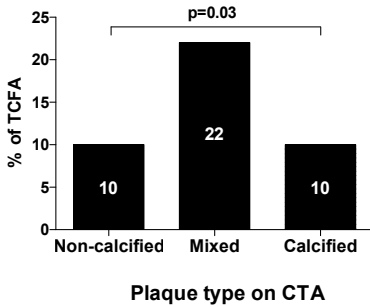


Figure 3. Comparison of presence (%) of thin cap fibroatheroma (TCFA) between the different plaque types on 320-row multidetector computed tomography angiography (CTA). Significantly more TCFA were present in mixed plaques (22%) as compared to non-calcified (10%) and calcified plaque (10%).

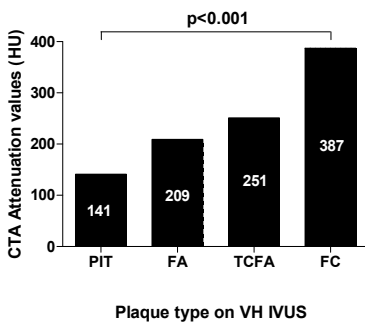


Figure 4. Comparison of attenuation values as measured in Hounsfield Units (HU) on 320-row multidetector computed tomography (CTA) between the different plaque types on virtual histology intravascular ultrasound (VH IVUS). A significant increase in CTA attenuation values is demonstrated for the more advanced plaque on VH IVUS. PIT, pathological intimal thickening; FA, fibroatheroma; TCFA, thin cap fibroatheroma; FC, fibrocalcific plaque.

ments of mixed plaques (258 ± 219 HU) on CTA paralleled average attenuation values of TCFA (251 ± 222 HU) on VH IVUS.

DISCUSSION

The present study evaluated the ability of plaque characterization on 320-row CTA as compared to invasive VH IVUS. In summary, the findings of the present study demonstrated that plaque characterization on 320-row CTA showed a good correlation with VH IVUS plaque characteristics. First, non-calcified plaques on 320-row CTA contained significantly more fibrotic tissue on VH IVUS than calcified plaques and mixed plaques on CTA. In addition, dense calcium on VH IVUS was most often observed in calcified plaques on CTA. Importantly, the highest amount of necrotic core (the more vulnerable plaque component) on VH IVUS was demonstrated in mixed plaque on 320-row CTA. Of particular interest was the finding that TCFA were most prevalent in mixed plaques, suggesting a possible higher degree of vulnerability in mixed plaques on CTA.

Second, the more advanced plaque types on VH IVUS corresponded to higher CTA attenuation values. Interestingly, CTA attenuation values of the more vulnerable plaque type (TCFA) on VH IVUS paralleled CTA attenuation values of the mixed plaques on 320-row CTA. However, these values still substantially overlapped as reflected by the large

standard deviations. Thus, distinction between the more subtle plaque features using CTA attenuation values does not seem feasible at this time.

Although 320-row CTA has only recently been introduced, preliminary data are available concerning the diagnostic performance of 320-row CTA.²⁰ De Graaf et al recently evaluated the diagnostic accuracy of 320-row CTA for detection of significant stenosis (defined as $\geq 50\%$ luminal narrowing) in 64 patients using quantitative coronary angiography as the reference of standard.⁶ The authors demonstrated an excellent diagnostic accuracy of 320-row for detection of significant stenosis, reporting sensitivity, specificity, and positive and negative predictive values on a patient basis of 100%, 88%, 92%, and 100%, respectively. Dewey et al also assessed the diagnostic accuracy 320-row CTA as compared to conventional coronary angiography in 30 patients.⁷ The authors concluded that 320-row CTA has a high diagnostic accuracy for detection of significant stenosis while significantly reducing radiation dose.

The main advantage of the 320-row CTA, as compared to 64-row CTA, is the 16 cm anatomical coverage that can cover an entire organ, such as the heart, in a single gantry rotation. Indeed, 320-row CTA can accurately acquire images of the heart in a single beat (350 ms) as compared to the typical 6-10 seconds needed for 64-row systems.²¹ Accordingly, this approach does not only lead to a marked reduction in radiation dose, it also eliminates helical acquisition artifacts. Additionally, due to the volume scanning approach, contrast is more homogeneously distributed through the coronary arteries, thereby potentially improving the ability and reliability to characterize plaque composition with 320-row CTA. Nevertheless, the temporal (175 ms) and spatial resolution (0.5 mm) of the 320-row CTA systems remain similar to the latest generation 64-row CTA systems.²¹

Regarding plaque observations with CTA, several previous studies have correlated plaque composition on CTA to plaque characteristics on invasive IVUS. Initially, Pohle et al compared plaque composition on 16-row CTA to grayscale intravascular ultrasound in 32 patients.²² The investigators identified 252 sites with non-calcified plaques on CTA and correlated the CTA attenuation values with invasive IVUS plaque characteristics. Interestingly, differences between subtle plaque features such as the more "vulnerable" lipid rich plaque (mean attenuation value of 58 ± 43 HU) and the more "stable" fibrous plaque (mean attenuation value of 121 ± 34 HU) were demonstrated, although the overlap of attenuation values between individual characteristics were still substantial. Consequently, over the years newer generation CTA systems have been introduced with improved spatial and temporal resolution. Amongst others, Sun et al evaluated plaque characterization on 64-row CTA.²³ The investigators studied 26 patients with 40 lesions that underwent both 64-row CTA and IVUS and observed that although CTA was able to distinguish between fibrous and calcified plaques to a significant degree, there was no difference between lipid rich (mean attenuation value of 79 ± 34 HU) and fibrous plaque components (mean attenuation value of 90 ± 27 HU). When compared to histology, Chopard et al also demonstrated that differentiation between fibrous and lipid rich plaques with grayscale IVUS and 64-row CTA still remained limited.²⁴

Only limited data are available regarding plaque composition assessment with VH IVUS in relation to CTA. In our institution, a previous comparison was made between CTA and VH IVUS, regarding the difference in plaque composition and vulnerability between lesions with significant ($\geq 50\%$ luminal narrowing) and non-significant stenosis on invasive coronary angiography in 78 patients. Interestingly, no evident relation existed between the degree of stenosis and plaque composition or vulnerability, as evaluated by CTA and VH IVUS.²⁵ In addition, Pundziute et al compared plaque composition between 64-row CTA and VH IVUS in 50 patients with 168 lesions.²⁶ Parallel to the current findings, the investigators also observed a good correlation between CTA and VH IVUS and demonstrated that TCFA was most often present in mixed plaque on CTA. However, the authors observed the largest amount of necrotic core in plaques deemed to be fully calcified on CTA, whereas in the current study necrotic core was largest in mixed plaques. This discrepancy can be possibly explained by differences in resolution between 64-row and 320-row CTA. Indeed, due to improved image quality, 320-row CTA could be superior in differentiating non-calcified elements within presence of calcified elements than 64-row CTA and thus allow more refined plaque characterization. Of note, dual-source CTA systems have recently been introduced that can operate two X-ray tubes at different kV settings. Accordingly, this may lead to more comprehensive characterization of atherosclerotic plaque, in particular the more calcified plaques.²⁷

Several histopathological studies have observed that high-risk plaque features include the presence of a large necrotic core and thin fibrous cap (TCFA).^{19,28,29} Indeed, the rupture of TCFA is thought to be the primary cause of ACS. There is an emerging need for imaging modalities that can identify atherosclerotic plaques with high-risk features, thus improving identification of patients that are at increased risk for events. In vivo, Rodriguez-Granillo et al demonstrated that VH IVUS was able to observe a higher degree of necrotic core and presence of TCFA in ACS patients as compared to patients with stable CAD.³⁰ In addition, VH IVUS could identify significantly more necrotic core in culprit lesions of patients presenting with ACS. However, VH IVUS is an invasive technique, restricted to patients referred for invasive coronary angiography and interventional procedures. Thus, a non-invasive modality that can identify patients at high risk would be preferred. Therefore, a number of previous studies have evaluated which plaque characteristics on CTA were related to increased plaque vulnerability. For instance, Pundziute et al compared plaque features on CTA between patients presenting with ACS and stable CAD and showed that mixed plaques were more prevalent in patients with ACS.³¹ In addition, Motoyama et al compared plaque features of 38 patients with ACS to 33 patients with stable complaints.³² Interestingly, features of mixed plaques such as spotty calcification and low attenuation non-calcified plaque elements were more often observed in patients with ACS. Importantly, when assessing the predictive value of plaque characteristics on CTA, the same authors demonstrated that these features (spotty calcifications, positive remodeling and low attenuation non-calcified plaque) were also prospectively related to the occurrence of ACS.³³ The aforementioned findings are in line with previous observations by IVUS suggesting that lesions containing smaller calcium deposits rather than extensive

calcifications are more often present in plaques related to ACS.^{34 35} Of note, concerning the prognostic value of plaque composition on CTA, Pundziute et al demonstrated that mixed plaques were associated with more adverse events during follow-up.³⁶ Accordingly, these observations as well as our current findings further support the notion that lesions classified as mixed on CTA may have a higher likelihood of vulnerability.

However, with the latest generation 320-row CTA scanners, exact characterization of the lipid core and thin fibrous cap is not feasible at the moment. Nonetheless, although direct identification of TCFA may not be possible, non-invasive techniques may still be valuable, as they may identify patients with a higher likelihood of having vulnerable plaques at a relatively early stage and may provide an opportunity for intensified treatment strategies.

Limitations

The following limitations of the present study should be considered. First, the present study only evaluated 62 patients in a single center. Ideally, a larger patient population should be studied, preferably in a multicenter setting. Secondly, CTA is related with ionizing radiation exposure. Therefore, patients and image protocols should be carefully selected to prevent unnecessary exposure to radiation. Thirdly, severe calcifications on CTA can cause beam hardening and blooming artifacts and as a result can influence plaque classification. Similarly on VH IVUS, due to acoustic shadowing, it is difficult to assess plaque composition behind severe calcifications. Therefore, possibly small non-calcified elements within the more heavily calcified parts of the plaque may have been missed. Fourthly, descriptive studies have reported the influence of luminal contrast-enhancement on plaque attenuation values. However, in the present study we did not adjust for intra-coronary lumen contrast-enhancement as there is currently no validated algorithm available for this purpose. Lastly, no quantitative measurements were performed on plaque assessed with 320-row CTA, such as plaque volume, length and remodeling index, however, currently new dedicated software techniques are being developed to facilitate these measurements in the future.

Conclusion

Plaque observations on 320-row CTA show good agreement to relative plaque composition on VH IVUS. Moreover, mixed plaques on 320-row CTA parallel the more high risk plaques on VH IVUS.

REFERENCES

1. Meijboom WB, Meijs MF, Schuijf JD et al. Diagnostic accuracy of 64-slice computed tomography coronary angiography: a prospective, multicenter, multivendor study. *J Am Coll Cardiol* 2008;52: 2135-44.
2. Miller JM, Rochitte CE, Dewey M et al. Diagnostic performance of coronary angiography by 64-row CT. *N Engl J Med* 2008;359:2324-36.
3. Mowatt G, Cook JA, Hillis GS et al. 64-Slice computed tomography angiography in the diagnosis and assessment of coronary artery disease: systematic review and meta-analysis. *Heart* 2008; 94:1386-93.
4. Schuijf JD, Beck T, Burgstahler C et al. Differences in plaque composition and distribution in stable coronary artery disease versus acute coronary syndromes; non-invasive evaluation with multi-slice computed tomography. *Acute Card Care* 2007;9:48-53.
5. Hein PA, Romano VC, Lembecke A et al. Initial experience with a chest pain protocol using 320-slice volume MDCT. *Eur Radiol* 2009;19:1148-55.
6. De Graaf FR, Schuijf JD, Van Velzen JE et al. Diagnostic accuracy of 320-row multidetector computed tomography coronary angiography in the non-invasive evaluation of significant coronary artery disease. *Eur Heart J* 2010.
7. Dewey M, Zimmermann E, Deissenrieder F et al. Noninvasive coronary angiography by 320-row computed tomography with lower radiation exposure and maintained diagnostic accuracy: comparison of results with cardiac catheterization in a head-to-head pilot investigation. *Circulation* 2009;120:867-75.
8. Steigner ML, Mitsouras D, Whitmore AG et al. Iodinated contrast opacification gradients in normal coronary arteries imaged with prospectively ECG-gated single heart beat 320-detector row computed tomography. *Circ Cardiovasc Imaging* 2010;3:179-86.
9. Hausleiter J, Meyer T, Hermann F et al. Estimated radiation dose associated with cardiac CT angiography. *JAMA* 2009;301:500-7.
10. De Graaf FR, Schuijf JD, Van Velzen JE et al. Diagnostic accuracy of 320-row multidetector computed tomography coronary angiography in the non-invasive evaluation of significant coronary artery disease. *Eur Heart J* 2010.
11. Austen WG, Edwards JE, Frye RL et al. A reporting system on patients evaluated for coronary artery disease. Report of the Ad Hoc Committee for Grading of Coronary Artery Disease, Council on Cardiovascular Surgery, American Heart Association. *Circulation* 1975;51:5-40.
12. Leber AW, Knez A, Becker A et al. Accuracy of multidetector spiral computed tomography in identifying and differentiating the composition of coronary atherosclerotic plaques: a comparative study with intracoronary ultrasound. *J Am Coll Cardiol* 2004;43:1241-7.
13. van der Giessen AG, Gijssen FJ, Wentzel JJ et al. Small coronary calcifications are not detectable by 64-slice contrast enhanced computed tomography. *Int J Cardiovasc Imaging* 2010.
14. Klass O, Kleinhans S, Walker MJ et al. Coronary plaque imaging with 256-slice Multidetector Computed Tomography: interobserver variability of volumetric lesion parameters with semiautomatic plaque analysis software. *Int J Cardiovasc Imaging* 2010;26:711-20.
15. Pundziute G, Schuijf JD, Van Velzen JE et al. Assessment with multi-slice computed tomography and gray-scale and virtual histology intravascular ultrasound of gender-specific differences in extent and composition of coronary atherosclerotic plaques in relation to age. *Am J Cardiol* 2010;105:480-6.
16. Mintz GS, Nissen SE, Anderson WD et al. American College of Cardiology Clinical Expert Consensus Document on Standards for Acquisition, Measurement and Reporting of Intravascular Ultrasound Studies (IVUS). A report of the American College of Cardiology Task Force on Clinical Expert Consensus Documents. *J Am Coll Cardiol* 2001;37:1478-92.

17. Nasu K, Tsuchikane E, Katoh O et al. Accuracy of in vivo coronary plaque morphology assessment: a validation study of in vivo virtual histology compared with in vitro histopathology. *J Am Coll Cardiol* 2006;47:2405-12.
18. Carlier SG, Mintz GS, Stone GW. Imaging of atherosclerotic plaque using radiofrequency ultrasound signal processing. *J Nucl Cardiol* 2006;13:831-40.
19. Virmani R, Kolodgie FD, Burke AP et al. Lessons from sudden coronary death: a comprehensive morphological classification scheme for atherosclerotic lesions. *Arterioscler Thromb Vasc Biol* 2000;20:1262-75.
20. Rybicki FJ, Otero HJ, Steigner ML et al. Initial evaluation of coronary images from 320-detector row computed tomography. *Int J Cardiovasc Imaging* 2008;24:535-46.
21. Voros S. What are the potential advantages and disadvantages of volumetric CT scanning? *J Cardiovasc Comput Tomogr* 2009;3:67-70.
22. Pohle K, Achenbach S, Macneill B et al. Characterization of non-calcified coronary atherosclerotic plaque by multi-detector row CT: comparison to IVUS. *Atherosclerosis* 2007;190:174-80.
23. Sun J, Zhang Z, Lu B et al. Identification and quantification of coronary atherosclerotic plaques: a comparison of 64-MDCT and intravascular ultrasound. *AJR Am J Roentgenol* 2008;190:748-54.
24. Chopard R, Bousset L, Motreff P et al. How reliable are 40 MHz IVUS and 64-slice MDCT in characterizing coronary plaque composition? An ex vivo study with histopathological comparison. *Int J Cardiovasc Imaging* 2010;26:373-83.
25. Van Velzen JE, Schuijf JD, De Graaf FR et al. Plaque type and composition as evaluated non-invasively by MSCT angiography and invasively by VH IVUS in relation to the degree of stenosis. *Heart* 2009;95:1990-6.
26. Pundziute G, Schuijf JD, Jukema JW et al. Head-to-head comparison of coronary plaque evaluation between multislice computed tomography and intravascular ultrasound radiofrequency data analysis. *JACC Cardiovasc Interv* 2008;1:176-82.
27. Henzler T, Porubsky S, Kaye H et al. Attenuation-based characterization of coronary atherosclerotic plaque: Comparison of dual source and dual energy CT with single-source CT and histopathology. *Eur J Radiol* 2010.
28. Kolodgie FD. Pathologic assessment of the vulnerable human coronary plaque. *Heart* 2004;90:1385-91.
29. Virmani R, Burke AP, Kolodgie FD et al. Pathology of the thin-cap fibroatheroma: a type of vulnerable plaque. *J Intervent Cardiol* 2003;16:267-72.
30. Rodriguez-Granillo GA, Garcia-Garcia HM, Mc Fadden EP et al. In vivo intravascular ultrasound-derived thin-cap fibroatheroma detection using ultrasound radiofrequency data analysis. *Journal of the American College of Cardiology* 2005;46:2038-42.
31. Pundziute G, Schuijf JD, Jukema JW et al. Evaluation of plaque characteristics in acute coronary syndromes: non-invasive assessment with multi-slice computed tomography and invasive evaluation with intravascular ultrasound radiofrequency data analysis. *Eur Heart J* 2008;29:2373-81.
32. Motoyama S, Kondo T, Sarai M et al. Multislice computed tomographic characteristics of coronary lesions in acute coronary syndromes. *J Am Coll Cardiol* 2007;50:319-26.
33. Motoyama S, Sarai M, Harigaya H et al. Computed tomographic angiography characteristics of atherosclerotic plaques subsequently resulting in acute coronary syndrome. *J Am Coll Cardiol* 2009;54:49-57.
34. Beckman JA, Ganz J, Creager MA et al. Relationship of clinical presentation and calcification of culprit coronary artery stenoses. *Arterioscler Thromb Vasc Biol* 2001;21:1618-22.
35. Ehara S, Kobayashi Y, Yoshiyama M et al. Spotty calcification typifies the culprit plaque in patients with acute myocardial infarction: an intravascular ultrasound study. *Circulation* 2004;110:3424-9.
36. Pundziute G, Schuijf JD, Jukema JW et al. Prognostic value of multislice computed tomography coronary angiography in patients with known or suspected coronary artery disease. *J Am Coll Cardiol* 2007;49:62-70.

